


Article

A Novel Co-Phase Power Supply System for Electrified Railway Based on V Type Connection Traction Transformer

Shaofeng Xie *, Yiming Zhang  and Hui Wang

School of Electrical Engineering, Southwest Jiaotong University, Chengdu 611756, China; ymzhang@my.swjtu.edu.cn (Y.Z.); huiwang@my.swjtu.edu.cn (H.W.)

* Correspondence: sfxie@swjtu.cn

Abstract: Power quality and neutral section are two technical problems that hinder the development of electrified railway to high-speed and heavy railway. The co-phase power supply technology is one of the best ways to solve these two technical problems. At present, a V type connection traction transformer is widely used in a power frequency single-phase AC traction power supply system, especially in high-speed railway. In this paper, a new type of co-phase power supply system for electrified railway based on V type connection traction transformer is proposed. One single-phase winding in the V type connection traction transformer is used as main power supply channel, and three ports are used as compensation ports. Neutral section is no longer set with traction substation, and the train is continuously powered through. The independent single-phase Static Var Generators (SVGs) are used to compensate the three-phase imbalance caused by single-phase traction load. When necessary, the power factor can be improved at the same time. The principle, structure, control strategy, and capacity configuration of the technical scheme are analyzed in this paper, and the effectiveness of the scheme is verified by using the measured data of electrified railway. The advantage of this scheme lies in the universal applicability of the V type connection traction transformer, and the flexibility of the SVG device.

Keywords: co-phase power supply technology; power quality; V type connection traction transformer; comprehensive compensation; Static Var Generator (SVG)



Citation: Xie, S.; Zhang, Y.; Wang, H. A Novel Co-Phase Power Supply System for Electrified Railway Based on V Type Connection Traction Transformer. *Energies* **2021**, *14*, 1214. <https://doi.org/10.3390/en14041214>

Academic Editors: Andrea Mariscotti and Leonardo Sandrolini

Received: 12 January 2021

Accepted: 19 February 2021

Published: 23 February 2021

Publisher's Note: MDPI stays neutral with regard to jurisdictional claims in published maps and institutional affiliations.



Copyright: © 2021 by the authors. Licensee MDPI, Basel, Switzerland. This article is an open access article distributed under the terms and conditions of the Creative Commons Attribution (CC BY) license (<https://creativecommons.org/licenses/by/4.0/>).

1. Introduction

As the backbone of modern comprehensive transportation system and one of the main modes of transportation, railway plays an important role in the process of social and economic development in China [1,2]. According to the railway statistics bulletin of 2019 issued by the State Railway Administration of China, by the end of 2019, business mileage has reached 139,000 km, and the railway electrification rate reached 71.9% [3].

With the development of electrified railways, power quality has always been a research hotspot, because of the characteristics of the traction power supply system [4]. A power frequency single phase AC system is widely used in China's electrified railways. The structure diagram of existing electrified railways is shown in Figure 1. As a single-phase power load essentially, traction load will cause power quality problems including mainly negative sequence in three-phase power system [5–7]. In order to reduce the influence of traction load on the three-phase unbalance at the Point of Common Coupling (PCC) of power system, the scheme of supplying power by sections in traction network and each section using three-phase power system in turn is usually adopted. The neutral section is set between two adjacent power supply sections [8–10]. However, it brings about a series of problems, such as the reduction of train speed, loss of traction force, frequent action of phase passing device, short service life, and low reliability, which seriously affect the safe and stable operation of the train. It shows that the neutral section is the weakest link in the AC traction power supply system of electric railway, and greatly restricts the traction power supply system Railway Development [11,12].

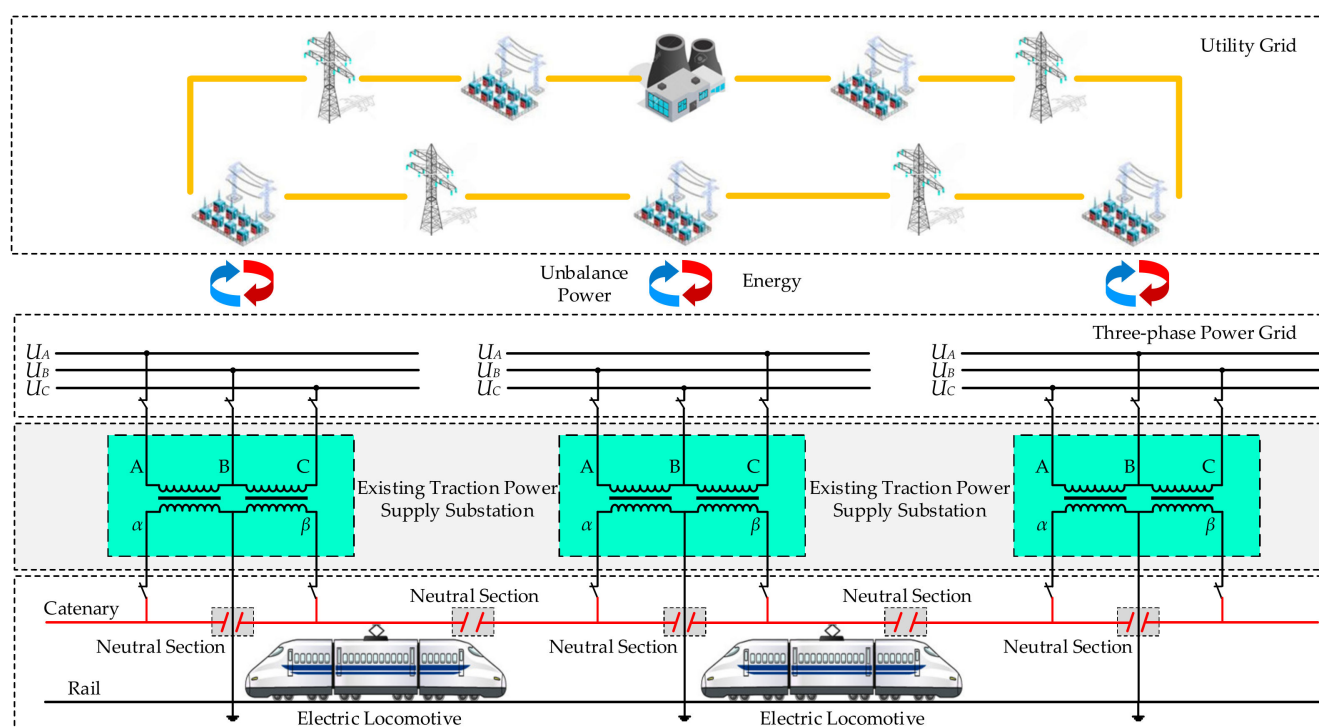


Figure 1. Structure diagram of China's existing traction power supply system.

With widespread use of AC-DC-AC electric locomotives using Pulse Width Modulation (PWM) technology, compared to the traditional AC-DC electric locomotives, the harmonic problem has been greatly improved, and the power factor is close to 1, which has overcome the shortcomings of traditional AC-DC electric locomotives [13–18]. However, at the same time, because of the huge increase in traction power of AC-DC-AC electric locomotives, the high-power single-phase traction load will cause more three-phase unbalance problems in the power system. Therefore, negative sequence will become the focus of power quality research of electrified railways.

In view of how to effectively solve the power quality problems including mainly negative sequence and neutral section, a lot of research work has been carried out, and different solutions have been put forward. The scheme to solve the negative sequence and electrical phase separation in Germany is adopting special railway power generation, transmission, and distribution system and setting a three-phase/single AC-DC-AC converter in the traction substation. At the same time, the neutral section is cancelled [19]. In Japan, Scott traction transformer and Railway Static Power Conditioner (RPC) are used in Shinkansen to compensate three-phase unbalance and voltage fluctuation so as to reduce the influence of traction load on three-phase power system [20–22]. It can solve the problem of power quality, and automatic passing neutral section technology is used to solve the problems caused by neutral section. Bilateral power supply technology is adopted in Russia to cancel neutral section between traction substations [19]. However, the traction power supply system is parallel with the power system transmission lines, and maybe there is current power in the traction power supply system, which needs to be restrained.

The idea of a co-phase power supply system to eliminate the neutral section and solve power quality problem is first proposed in [23]. The co-phase power supply refers to the power supply mode that a traction substation or multiple traction substations of a railway line supply the whole traction network with the same phase (line) voltage in the same three-phase power grid. If two adjacent traction substations adopt bilateral power supply, the co-phase power supply network formed by multiple traction substations on the line is called through co-phase power supply, referred to as through power supply [24,25].

Since the concept of co-phase power supply system was proposed, there have been some related studies on topological structure, compensation technology, and control strategy about co-phase power supply system. The co-phase power supply scheme based on three-phase-two-phase balanced connection traction transformer and Power Flow Controller (PFC) is proposed in [26]. Furthermore, more co-phase power supply schemes are proposed in [19,27,28]. Moreover, the schemes proposed in [19,26] have been applied in the Meishan traction substation of Chengdu Kunming railway, Shayu traction substation of Central South Passage of Shanxi Province, and Wenzhou City railway S1 line. The practice results show that the co-phase power supply technology can effectively solve the power quality problem with negative sequence as the main factor and cancel the neutral section at the traction substation.

In order to effectively reduce the PFC device capacity, a co-phase power supply scheme based on Hybrid Power Quality Conditioner (HPQC) was proposed in [29]. By using relatively inexpensive passive components to provide a part of reactive power, the active device capacity can be reduced. In order to obtain satisfactory compensation effects, the HPQC system often needs to consider more complex factors in design. A scheme to reduce the device capacity of RPC by using a C-type filter is proposed in [30], the C-type filter can compensate for a part of reactive power of the traction load while filtering out harmonics. Therefore, the device capacity of RPC can be reduced to a certain extent. In addition, based on the Modular Multilevel Converter (MMC) technology, the co-phase power supply schemes by using three-phase/single-phase AC-DC-AC converter is introduced in [31–33]. The outstanding advantage of these design schemes is that they can realize the balanced transformation between a three-phase system and single-phase system without generating power quality problems. However, it should be noted that in these schemes, all the power of the traction load will be transmitted through the power electronic converter, so the required device capacity will be equivalent to the capacity of a traditional traction transformer [34].

In recent years, Static Var Generator (SVG) has been widely used in various transmission and distribution systems due to its outstanding performance in compensating reactive power, etc. [35]. Compared with the traditional Static Var Compensator (SVC), SVG has the characteristics of faster dynamic response and lower harmonic content [36–38].

In view of this, a co-phase power supply scheme based on SVG for V type connection traction transformer which is widely used in high-speed railway is proposed in this paper. The feature of the scheme is that the traction load and compensation equipment share the same transformer, which can realize the comprehensive compensation of negative sequence and reactive power, effectively solve the problem of power quality, and cancel the neutral section at traction substation. Furthermore, the capacity of compensation equipment is minimized.

2. System Structure

Based on V type connection traction transformer and SVG, a novel co-phase power supply system for electrified railway is proposed in this paper. By means of unequal side V type connection traction transformer and setting single-phase SVG on multiple ports of the secondary side, the negative sequence and reactive power comprehensive compensation is carried out for three-phase unbalance and power factor, so that the power quality can meet the standard. For traction load, neutral section at the outlet of traction substation can be cancelled to realize co-phase power supply. The scheme of system is shown in Figure 2.

In Figure 2, the system mainly includes the Traction Compensation Transformer (TCT), the Comprehensive Compensation Equipment (CCE), and the Measurement and Control System (MCS). TCT is composed of unequal side V type connection traction transformer. The primary side terminal of TCT is connected with three-phase power system. The secondary side port ab of TCT is traction port, and port ac, b'c, and ad are compensation ports.

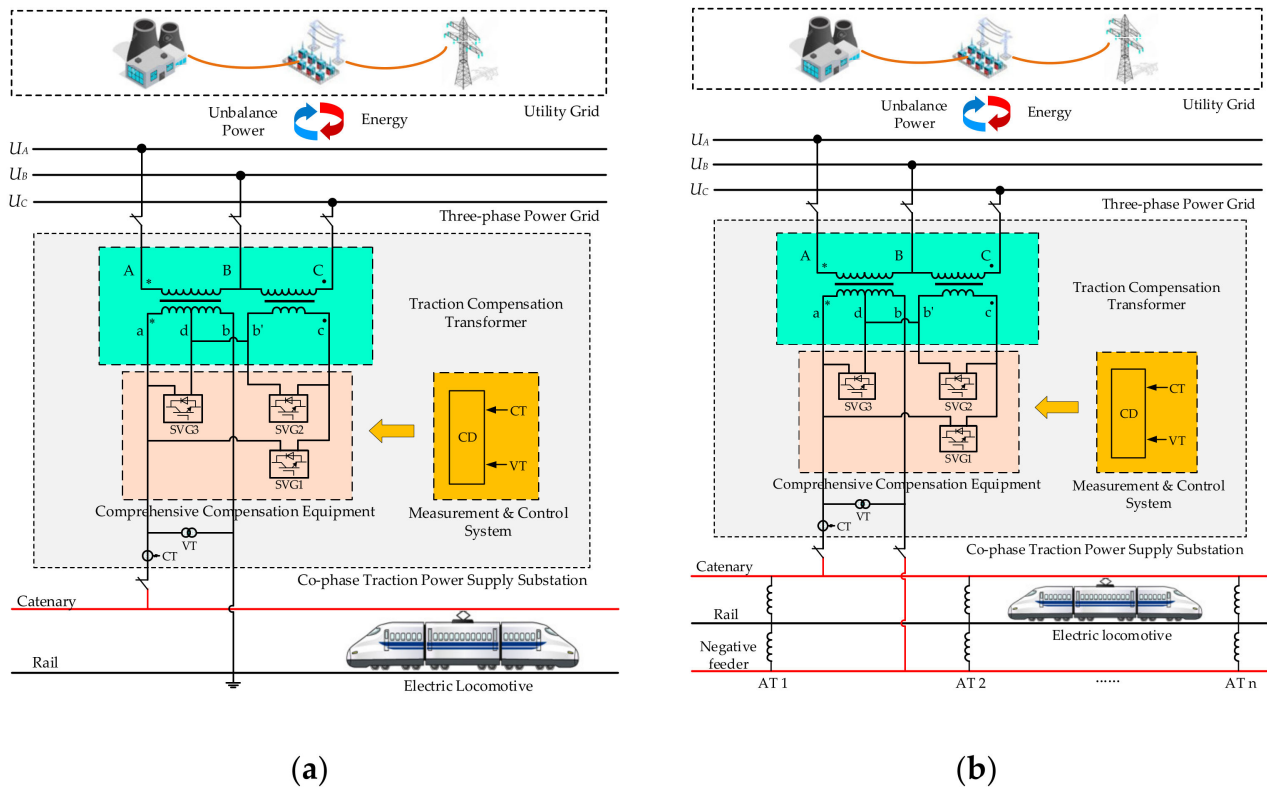


Figure 2. Structure diagram of traction substation with co-phase power supply. (a) Traction substation under direct power supply mode; (b) traction substation under Auto Transformer (AT) power supply mode.

CCE is composed of three single-phase SVGs, which are connected with compensation ports, respectively. MCS includes the Voltage Transformer (VT), the Current Transformer (CT), and the Controller Device (CD), and the signal output terminal of CD is connected with the control terminal of CCE.

Traction port ab of TCT is connected to traction network with VT and CT. If the power supply mode of traction network is direct power supply mode or direct power supply mode with return line, as shown in Figure 2a, terminal a of traction port ab is connected with traction network, terminal b is connected with rail.

If the traction network power supply mode is AT power supply mode, as shown in Figure 2b, terminal a of traction port ab of TCT is connected with traction network, and terminal b is connected with negative feeder.

3. Comprehensive Compensation Principle

The system takes the negative sequence limits of three-phase high-voltage bus and power factor as the compensation target. By controlling the reactive power generated by CCE, the reactive power and negative sequence generated by single-phase traction load are comprehensively compensated, so that the compensated power factor and negative sequence meet the requirements of the compensation target. CCE only changes the reactive power flow and does not change the active power flow.

3.1. Comprehensive Compensation Principle

According to reference [39], any traction port or compensation port λ on the secondary side of the traction transformer, the positive and negative sequence currents i_{λ}^{+} and i_{λ}^{-} generated on the primary side can be expressed as

$$\begin{cases} \dot{I}_\lambda^+ = \frac{1}{\sqrt{3}} k_\lambda I_\lambda e^{-j\phi_\lambda} \\ \dot{I}_\lambda^- = \frac{1}{\sqrt{3}} k_\lambda I_\lambda e^{-j(2\psi_\lambda + \phi_\lambda)} \end{cases} \quad (1)$$

where I_λ is the effective value of the port current; ψ_λ is the angle at which \dot{U}_λ lags \dot{U}_A ; ϕ_λ is the power factor angle; $k_\lambda = U_\lambda / \sqrt{3} U_A$. U_λ is the effective value of the port voltage \dot{U}_λ .

The traction load current and power factor angle of TCT secondary traction port are set as \dot{I}_L and ϕ_L , respectively. Taking the traction load in traction condition as an example, the comprehensive compensation principle of CCE is analyzed as follows.

When CCE performs comprehensive compensation, its positive and negative sequence phasor diagram is shown in Figure 3.

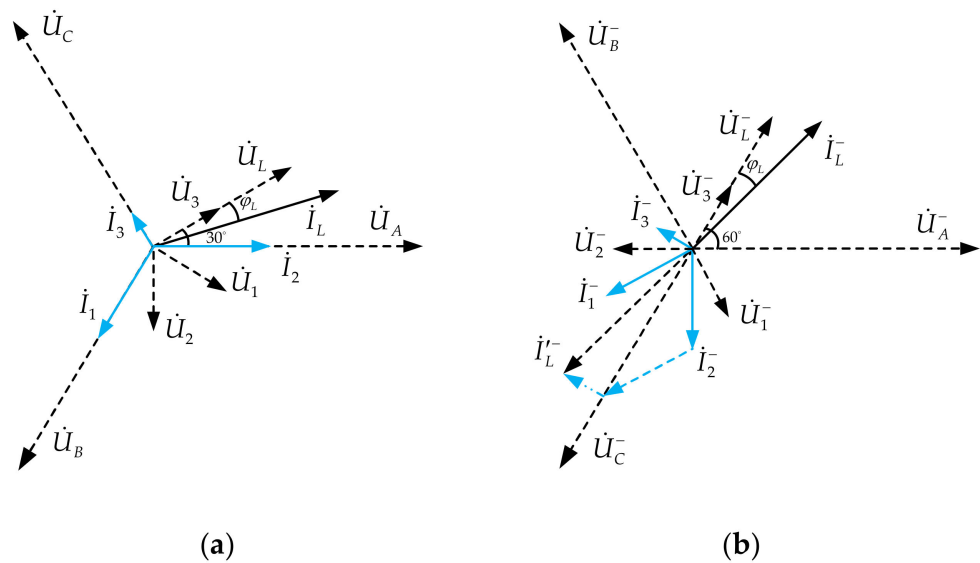


Figure 3. Phasor diagram of comprehensive compensation principle. (a) Phasor diagram of Positive sequence; (b) phasor diagram of Negative sequence.

In Figure 3, \dot{U}_A , \dot{U}_B , and \dot{U}_C are the A, B, C three-phase voltage of the three-phase high-voltage bus, and \dot{U}_1 , \dot{U}_2 , and \dot{U}_3 are the compensation port voltage of TCT secondary side SVG1, SVG2, and SVG3, respectively, and \dot{U}_L is the traction port voltage of the TCT secondary side. The corresponding negative sequence voltage are \dot{U}_A^- , \dot{U}_B^- , \dot{U}_C^- , \dot{U}_1^- , \dot{U}_2^- , \dot{U}_3^- , and \dot{U}_L^- . According to the topology of CCE, the relation diagram of positive sequence phasor and negative sequence phasor can be determined. Furthermore, the reactive currents generated by SVG1, SVG2, and SVG3 are \dot{I}_1 , \dot{I}_2 , and \dot{I}_3 , respectively, where \dot{I}_1 is inductive current and \dot{I}_2 and \dot{I}_3 are capacitive current. The corresponding negative sequence currents are \dot{I}_1^- , \dot{I}_2^- , and \dot{I}_3^- , respectively. The resultant negative sequence current $\dot{I}_L'^-$ can be used to offset the negative sequence current \dot{I}_L^- generated by the traction load. When the negative sequence is fully compensated, Equation (2) is correct:

$$\dot{I}_L^- + \dot{I}_L'^- = \dot{I}_L^- + \dot{I}_1^- + \dot{I}_2^- + \dot{I}_3^- = 0. \quad (2)$$

3.2. Comprehensive Compensation Model

According to the above analysis, it can be seen that CCE compensates the negative sequence and reactive power compensation simultaneously. Generally, the check point of negative sequence and power factor is Point of Common Coupling (PCC), so the negative sequence and reactive power generated by traction load at PCC are compensation object.

In case of CCE compensation, the active power of traction load remains unchanged at PCC, then reactive power Q_{CSS} and power factor $\cos \phi'_L$ after compensation can be expressed as follows:

$$Q_{CSS} = S_L \sin \phi_L + \sum_{k=1}^n S_k \sin \phi_k = (1 - K_C) S_L \sin \phi_L, \quad (3)$$

$$\cos \phi'_L = \frac{S_L \cos \phi_L}{\sqrt{(S_L \cos \phi_L)^2 + (Q_{CSS})^2}}, \quad (4)$$

where S_L and ϕ_L are the total apparent power and power factor angle of traction load. S_k and ϕ_k are the reactive power and power factor angle of SVG, respectively. n is the number of compensation ports, so $n = 3$ for Figure 2. K_C is the reactive power compensation degree.

According to Equation (3), K_C can be expressed as

$$K_C = -\frac{\sum_{k=1}^n S_k \sin \phi_k}{S_L \sin \phi_L}. \quad (5)$$

After using CCE to compensate, the negative sequence power at PCC is

$$\dot{S}^- = S_L e^{j\theta_L} + \sum_{k=1}^n S_k e^{j\theta_k} = (1 - K_N) S_L e^{j\theta_L}, \quad (6)$$

where $\theta_L = 2\psi_L + \phi_L$, ψ_L , and ϕ_L are angle of \dot{U}_L lagging behind \dot{U}_A and traction load power factor angle; $\theta_k = 2\psi_k + \phi_k$, ψ_k , and ϕ_k are angle of compensating port k voltage lagging behind \dot{U}_A and power factor angle of SVG, respectively; K_N is the negative sequence compensation degree.

According to Equation (6), K_N can be expressed as

$$K_N = -\frac{\sum_{k=1}^n S_k e^{j\theta_k}}{S_L e^{j\theta_L}}. \quad (7)$$

According to Equations (5) and (7), the comprehensive compensation effects of reactive power and negative sequence can be determined respectively by K_C and K_N . K_C and K_N are real numbers, and the range is $K_C, K_N \in [0, 1]$.

Equation (7) is expanded according to the real part and the imaginary part, respectively, and constitutes the simultaneous equations together with Equation (5). The comprehensive compensation model shown as Equation (8):

$$\begin{cases} K_C S_L \sin \phi_L = -\sum_{k=1}^n S_k \sin \phi_k \\ K_N S_L \cos \theta_L = -\sum_{k=1}^n S_k \cos \theta_k \\ K_N S_L \sin \theta_L = -\sum_{k=1}^n S_k \sin \theta_k \end{cases}. \quad (8)$$

The reactive power generated by SVG1, SVG2, and SVG3 are S_1 , S_2 , and S_3 , respectively, and according to Section 3.1, $\phi_1 = \pi/2$, $\phi_2 = -\pi/2$, and $\phi_3 = -\pi/2$, the comprehensive compensation model can be obtained as follows according to Equation (8):

$$\begin{cases} K_C S_L \sin \phi_L = -S_1 + S_2 + S_3 \\ K_N S_L \cos(2\psi_L + \phi_L) = S_1 \sin 2\psi_1 - S_2 \sin 2\psi_2 - S_3 \sin 2\psi_3 \\ K_N S_L \sin(2\psi_L + \phi_L) = -S_1 \cos 2\psi_1 + S_2 \cos 2\psi_2 + S_3 \cos 2\psi_3 \end{cases}, \quad (9)$$

where $\psi_L = -\pi/6$, $\psi_1 = -5\pi/6$, $\psi_2 = -\pi/2$, and $\psi_3 = -\pi/6$.

S_1 , S_2 , and S_3 can be solved by Equation (9):

$$\begin{cases} S_1 = \frac{1}{\sqrt{3}} K_N S_L \cos \phi_L + \frac{1}{3} (K_N - K_C) S_L \sin \phi_L \\ S_2 = \frac{1}{\sqrt{3}} K_N S_L \cos \phi_L - \frac{1}{3} (K_N - K_C) S_L \sin \phi_L \\ S_3 = \frac{1}{3} (2K_N + K_C) S_L \sin \phi_L \end{cases}, \quad (10)$$

where $S_k > 0$ ($k = 1, 2$) means that SVG1 and SVG2 output inductive and capacitive reactive power, respectively; otherwise, SVG1 and SVG2 output capacitive and inductive reactive power, respectively; SVG3 always output capacitive reactive power.

If Equation (10) is divided by U_L , the reactive current generated by SVG1, SVG2, and SVG3 are shown in Equation (11):

$$\begin{cases} I_1 = \frac{k_M}{\sqrt{3}k_L} \left[K_N I_L \cos \phi_L + \frac{1}{\sqrt{3}} (K_N - K_C) I_L \sin \phi_L \right] \\ I_2 = \frac{k_M}{\sqrt{3}k_L} \left[K_N I_L \cos \phi_L - \frac{1}{\sqrt{3}} (K_N - K_C) I_L \sin \phi_L \right] \\ I_3 = \frac{k_M}{3k_L} (2K_N + K_C) I_L \sin \phi_L \end{cases}, \quad (11)$$

where $k_L = \sqrt{3}U_A/U_L$, $k_M = \sqrt{3}U_A/U_k$ ($k = 1, 2, 3$), and satisfies $U_1 = U_2 = U_3$.

4. Comprehensive Compensation Control Strategy

As shown in Figure 4, set the instantaneous value of voltage on primary side of TCT as $U_A(t) = \sqrt{2}U_A \sin(\omega t)$. With \dot{U}_A as the reference, the port voltage of traction port \dot{U}_L and load current \dot{I}_L are shown as follows:

$$U_L(t) = \sqrt{2}U_L \sin(\omega t - \psi_L) = \sqrt{2}U_L \sin(\omega t + \frac{\pi}{6}), \quad (12)$$

$$I_L(t) = I_{L1}(t) + I_{Lh}(t) = \sqrt{2}I_{L1} \sin(\omega t + \frac{\pi}{6} - \phi_{L1}) + I_{Lh}(t), \quad (13)$$

where $I_{L1}(t)$ is the fundamental current; $I_{Lh}(t)$ is the harmonic current; I_{L1} is the effective value of the fundamental current; ω is the angular frequency; and ϕ_{L1} is the fundamental power factor angle. The fundamental component I_{L1} of load current can be further decomposed into instantaneous active component I_{L1p} and instantaneous reactive component I_{L1q} :

$$I_{L1}(t) = \sqrt{2}I_{L1p} \sin(\omega t + \frac{\pi}{6}) - j\sqrt{2}I_{L1q} \cos(\omega t + \frac{\pi}{6}), \quad (14)$$

where $I_{L1p} = I_{L1} \cos \phi_L$, $I_{L1q} = I_{L1} \sin \phi_L$.

By introducing Equation (14) into Equation (13) and multiplying both sides of the equation by $\sin(\omega t + \frac{\pi}{6})$ and $\cos(\omega t + \frac{\pi}{6})$, Equations (15) and (16) can be obtained:

$$I_L(t) \sin(\omega t + \frac{\pi}{6}) = \left[\frac{\sqrt{2}}{2} I_{L1p} - \frac{\sqrt{2}}{2} I_{L1p} \cos(2\omega t + \frac{\pi}{3}) - \frac{\sqrt{2}}{2} I_{L1q} \sin(2\omega t + \frac{\pi}{3}) \right] + I_{Lh}(t) \sin(\omega t + \frac{\pi}{6}), \quad (15)$$

$$I_L(t) \cos(\omega t + \frac{\pi}{6}) = \left[-\frac{\sqrt{2}}{2} I_{L1q} + \frac{\sqrt{2}}{2} I_{L1q} \cos(2\omega t + \frac{\pi}{3}) + \frac{\sqrt{2}}{2} I_{L1p} \sin(2\omega t + \frac{\pi}{3}) \right] + I_{Lh}(t) \cos(\omega t + \frac{\pi}{6}). \quad (16)$$

DC components $\frac{\sqrt{2}}{2} I_{L1p}$ and $-\frac{\sqrt{2}}{2} I_{L1q}$ can be separated from Equations (15) and (16), and then I_{L1p} and I_{L1q} can be obtained.

4.1. System Control Strategy

When CCE operates, \dot{U}_1 , \dot{U}_2 , and \dot{U}_3 are, respectively, locked by phase-locked loop (PLL) to generate synchronous signals $\sin(\omega t - \frac{\pi}{6})$, $\sin(\omega t - \frac{\pi}{2})$, and $\sin(\omega t + \frac{\pi}{6})$. Under the traction condition of traction load, SVG1 outputs inductive reactive power, SVG2 and SVG3 output capacitive reactive power. Therefore, the synchronous signals of compensation current of SVG1, SVG2, and SVG3 are, respectively, $-\cos(\omega t - \frac{\pi}{6})$, $\cos(\omega t - \frac{\pi}{2})$, and $\cos(\omega t + \frac{\pi}{6})$. According to Equation (11), the expected values of compensation current of SVG1, SVG2, and SVG3, I_1^* , I_2^* , and I_3^* are

$$\begin{cases} I_1^* = -\frac{\sqrt{2}k_M}{\sqrt{3}k_L} \left[K_N I_{L1p} + \frac{1}{\sqrt{3}} (K_N - K_C) I_{L1q} \right] \cos(\omega t - \frac{\pi}{6}) \\ I_2^* = \frac{\sqrt{2}k_M}{\sqrt{3}k_L} \left[K_N I_{L1p} - \frac{1}{\sqrt{3}} (K_N - K_C) I_{L1q} \right] \cos(\omega t - \frac{\pi}{2}) \\ I_3^* = \frac{\sqrt{2}k_M}{3k_L} [(2K_N + K_C) I_{L1q}] \cos(\omega t + \frac{\pi}{6}) \end{cases} \quad (17)$$

According to Equation (17), the block diagram of the expected value detection of compensation currents of the CCE is shown in Figure 5.

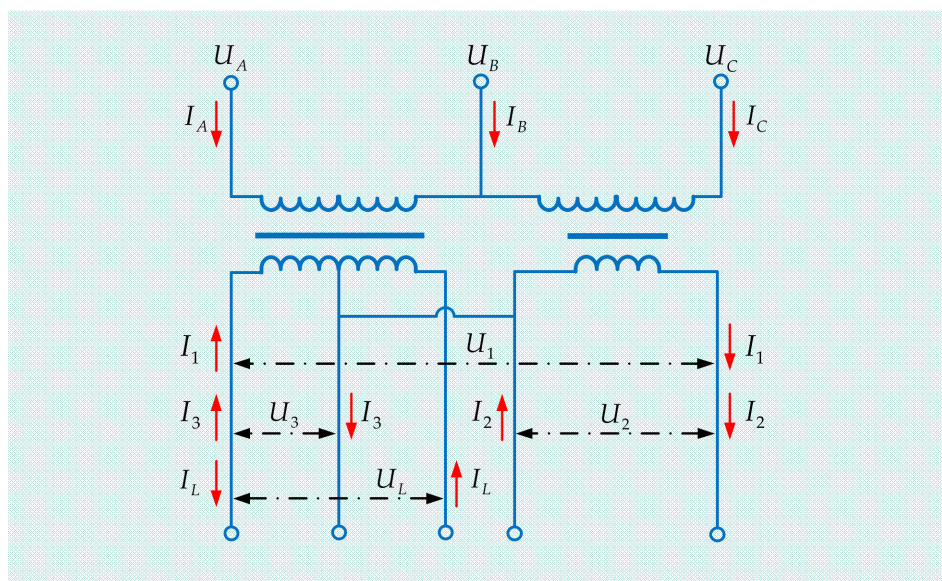


Figure 4. Simplified electrical schematic diagram of Traction Compensation Transformer (TCT).

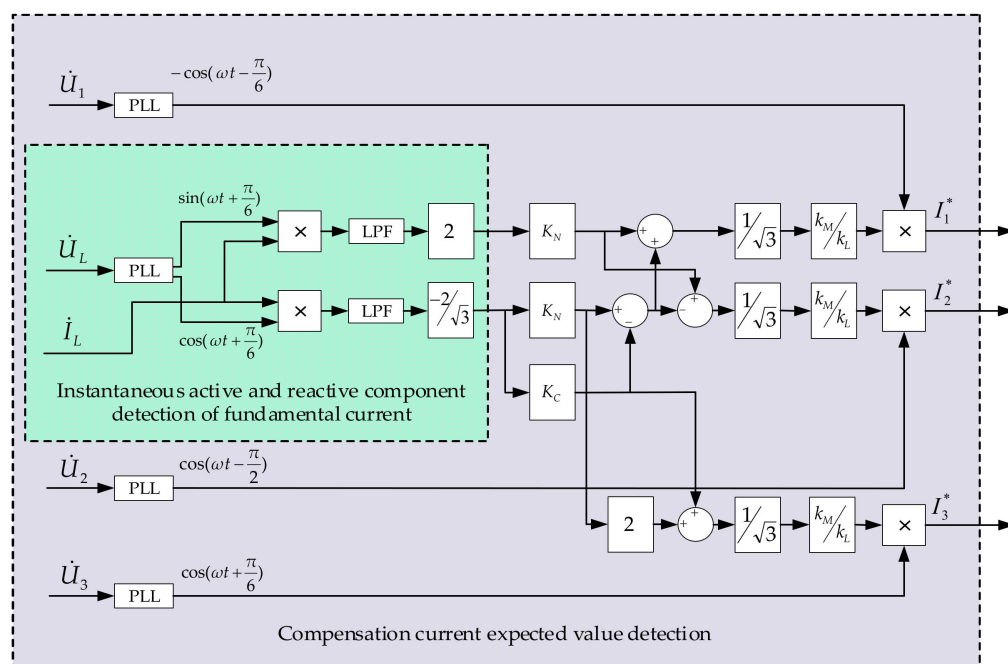


Figure 5. Block diagram of expected value detection of compensation currents.

The expected compensation currents I_1^* , I_2^* , and I_3^* are compared with the actual currents value I_1 , I_2 , and I_3 on the compensation port. After PI adjustment, the PWM control signal driving SVG is generated by carrier modulation technology. Therefore, the CCE can be controlled to send out the corresponding expected compensation currents. The control block diagram of CCE is shown in Figure 6.

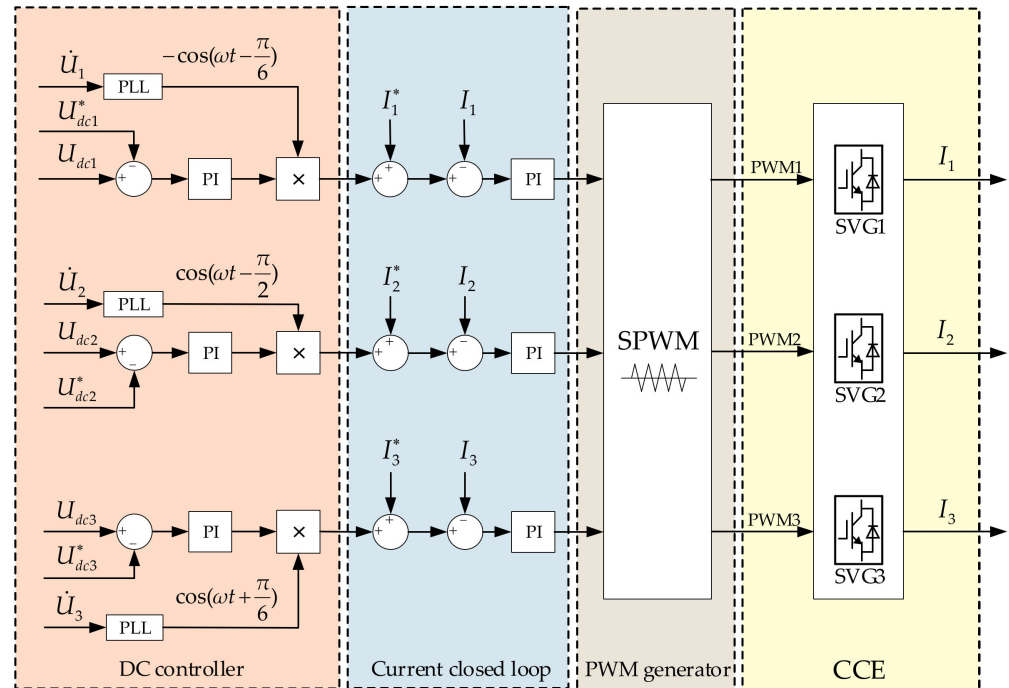


Figure 6. Control block diagram of Comprehensive Compensation Equipment (CCE).

4.2. Determination Method and Steps of K_C and K_N

In the integrated compensation control strategy, the key to achieve the compensation goal is to confirm the appropriate reactive power compensation degree K_C and negative sequence compensation degree K_N .

The relationship between the K_C and power factors can be obtained by solving Equations (3) and (4) simultaneously:

$$K_C = 1 - \sqrt{\frac{(\tan \phi'_L)^2}{(\tan \phi_L)^2}} = 1 - \sqrt{\frac{(\cos \phi'_L)^{-2} - 1}{(\cos \phi_L)^{-2} - 1}} \quad (18)$$

where $\cos \phi_L$ and $\cos \phi'_L$ are power factors before and after compensation.

The following relationship between the limit of three-phase voltage unbalance degree at PCC ε_{U2} and the allowable negative sequence power at PCC S_ε is

$$S_\varepsilon = \varepsilon_{U2} \cdot S_d, \quad (19)$$

where S_d is the short circuit capacity at PCC.

If the residual negative sequence power caused by traction load at PCC after compensation is \dot{S}^- , its magnitude shall meet $|\dot{S}^-| \leq S_\varepsilon$. The relationship between K_N and expected value of three-phase voltage unbalance degree ε_{U2}^* can be obtained by solving Equations (6) and (19), as shown in Equation (20):

$$K_N = \frac{S_L - \varepsilon_{U2}^* \cdot S_d}{S_L}. \quad (20)$$

At present, AC/DC/AC electric locomotive and AC/DC electric locomotive are widely used in electrified railway. According to load characteristics, the methods for determining the values of K_C and K_N can be summarized as follows, the specific steps are

- (1) When the negative sequence power S_L^- generated by the traction load is greater than the allowable negative sequence power S_e at PCC, and the power factor $\cos \phi_L$ is less than the target power factor value $\cos \phi^*$, the negative sequence and reactive power are compensated by CCE at the same time. Based on the expected target, the value of K_C and K_N can be determined according to Equations (18) and (20). Then, according to Equation (10), the S_1 , S_2 , and S_3 are obtained. Under the traction condition of traction load, S_1 is inductive or capacitive reactive ($S_1 > 0$ or $S_1 < 0$), S_2 is capacitive or inductive reactive ($S_2 > 0$ or $S_2 < 0$), and S_3 is capacitive reactive;
- (2) When S_L^- is greater than S_e , and $\cos \phi_L$ is greater than or equal to $\cos \phi^*$. Only the negative sequence power is compensated by CCE, and the power factor is not changed before and after compensation. Therefore, K_C can be determined by $K_C = 0$, and based on the expected target after compensation, the value of K_N can be determined according to Equation (20). Then according to Equation (10), the S_1 , S_2 , and S_3 are obtained. Under the traction condition of traction load, S_1 is inductive reactive, S_2 and S_3 are capacitive reactive;
- (3) When S_L^- is less than or equal to S_e , and $\cos \phi_L$ is less than $\cos \phi^*$. Only the reactive sequence power is compensated by CCE. Therefore, K_N can be determined by $K_N = 0$, and based on the expected target after compensation, the value of K_C can be determined according to Equation (18). Then, according to Equation (10), the S_1 , S_2 , and S_3 are obtained. Under the traction condition of traction load, S_1 , S_2 , and S_3 are all capacitive reactive;
- (4) When S_L^- is less than or equal to S_e , and $\cos \phi_L$ is greater than or equal to $\cos \phi^*$. The negative sequence and reactive power generated by the traction load can meet the compensation target, no additional compensation is required. Therefore, K_N and K_C can be determined by $K_N = 0$ and $K_C = 0$. CCE operates in standby.

In summary, the schematic diagram of the process of determining the values of K_C and K_N is shown in Figure 7.

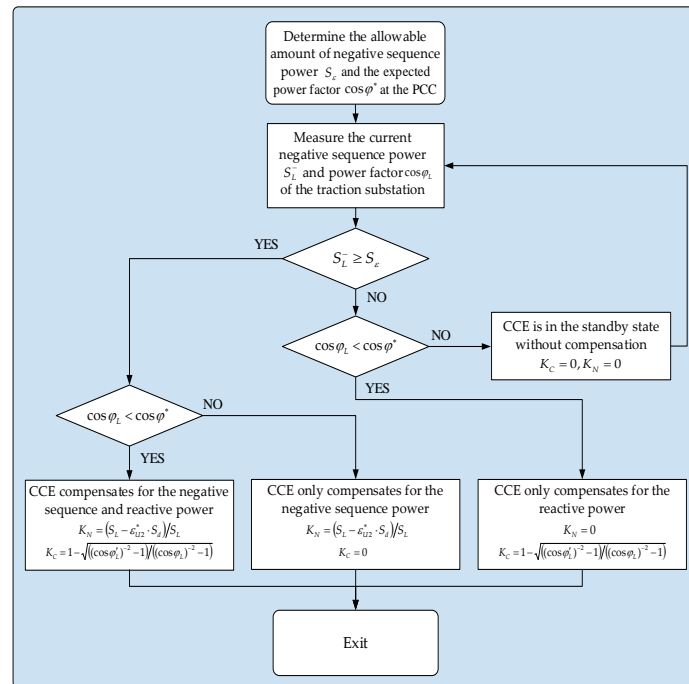


Figure 7. Schematic diagram of the process of determining the values of K_C and K_N .

5. Effectiveness Verification

5.1. Analysis and Verification of Comprehensive Compensation Scheme Based on Actual Case

Take the actual data of an electrified railway traction load as an example for illustration. The traction transformer is single-phase wiring, and its primary side is connected to the A and B phases of the 110 kV power system. The primary and secondary side transformation ratio is 110/27.5. By using the power quality test device, the amplitude and phase angle of the voltage and current of the primary and secondary sides of the traction transformer are recorded. The measurement period is 24 h. After processing the data, the diagram of 24-h load curve of the traction load is shown in Figure 8.

After further statistical analysis of the load data, it shows that the 95% probability value of the three-phase voltage unbalance degree of the traction substation is 1.2%, and the maximum is 3.6%. The maximum value has exceeded 2.6%, the limit of the three-phase voltage unbalance degree standard [40]. In addition, the daily average power factor of the traction substation is 0.79, which is lower than the economic power factor of 0.9 required by the power system. Therefore, it is necessary to set up an appropriate compensation scheme for comprehensive treatment of the negative sequence and reactive power in the traction substation. The diagram of 24-h three-phase voltage unbalance degree curve of the traction substation is shown in Figure 9.

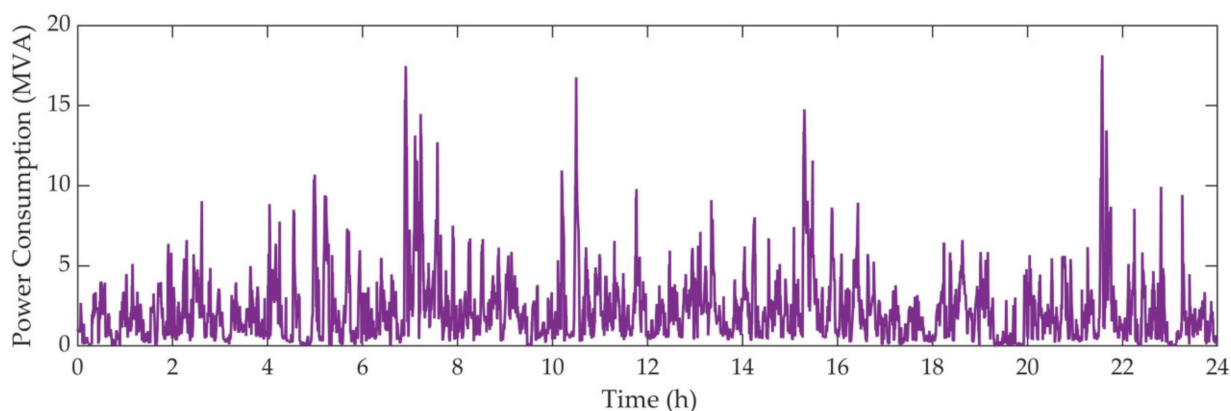


Figure 8. Diagram of 24-h load curve of the traction substation.

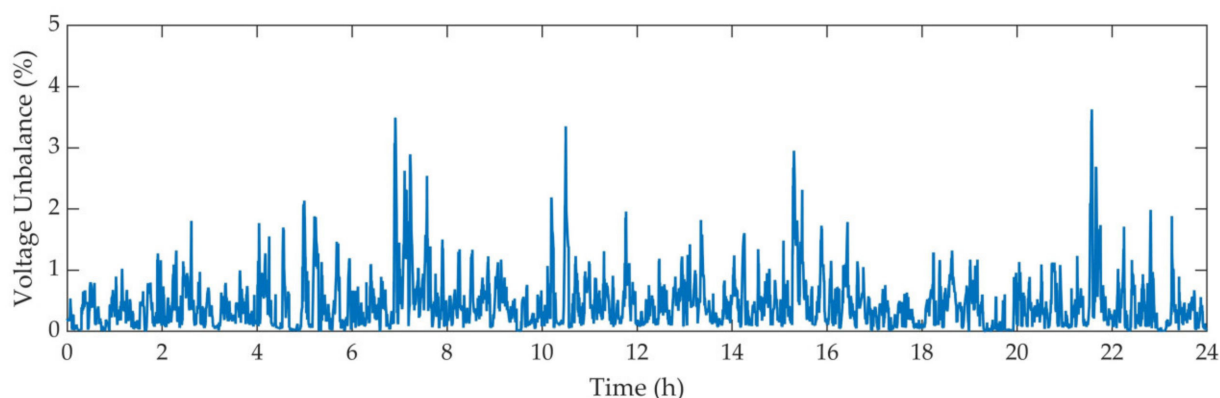


Figure 9. Diagram of 24-h three-phase voltage unbalance degree curve of the traction substation.

The design target of the compensation scheme proposed in this paper is that after compensation, the maximum value of the three-phase voltage unbalance degree of the traction substation will be reduced to a value less than the limit, for example, 2.5%, the 95% probability value will be further reduced to a value less than the limit, for example, 1%, and the daily average power factor is increased to 0.9.

In order to reduce the capacity of the compensation device as much as possible, for the condition where the three-phase voltage unbalance degree caused by the traction load is greater than 1.2%, the first negative sequence allowable amount $S_{\varepsilon 1}$ will implemented as the assessment reference value, $S_{\varepsilon 1} = 12.5$ MVA. According to Equation (19), it can be known that the corresponding three-phase voltage unbalance degree target is 2.5%. If S_L^- is greater than $S_{\varepsilon 1}$, the expected value of the three-phase voltage unbalance degree after compensation is set to 2.5%. Otherwise, S_L^- meets the requirements of $S_{\varepsilon 1}$, so that the CCE is standby. However, for the condition where the three-phase voltage unbalance degree is less than or equal to 1.2%, the allowable second negative sequence $S_{\varepsilon 2}$ will implemented as the assessment reference value, $S_{\varepsilon 2} = 5$ MVA. Moreover, the corresponding three-phase voltage unbalance degree target is 1.0%. If S_L^- is greater than $S_{\varepsilon 2}$, the expected value of the three-phase voltage unbalance degree after compensation is set to 1.0%. Otherwise, S_L^- meets the requirements of $S_{\varepsilon 2}$ and similarly there is also no need to compensate for the negative sequence power.

Based on the selection of the above limits, by using the determination method and steps of K_C and K_N given in Section 4.2, the values of K_C and K_N corresponding to the load at each moment of the traction substation can be calculated. As shown in Figure 10.

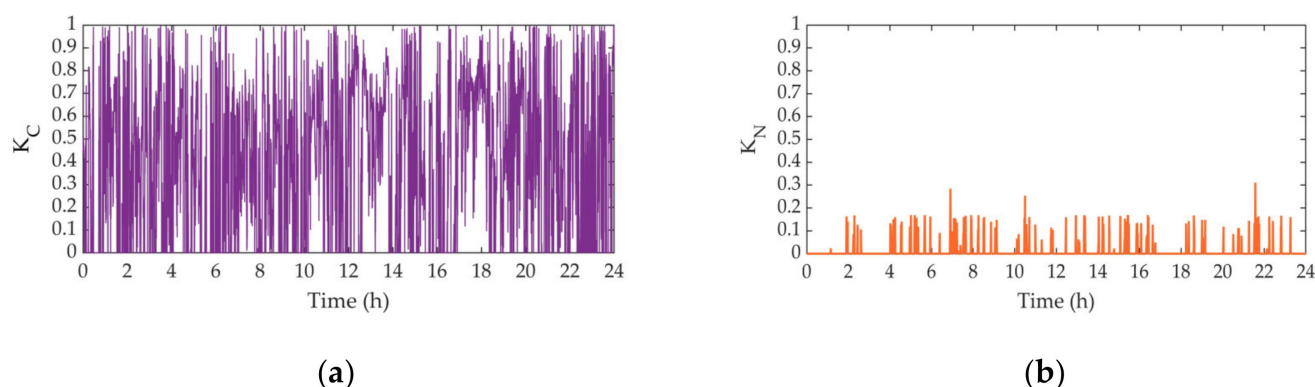


Figure 10. Diagram of 24-h K_C and K_N calculation results curve of the traction substation. (a) Diagram of calculation results for reactive power compensation degree K_C during a day; (b) diagram of calculation results for negative sequence compensation degree K_N during a day.

According to the calculation results of K_C and K_N in Figure 10, it can be further calculated by Equation (10) that the maximum reactive power compensation amount required by SVG1, SVG2, and SVG3 are 2.66 MVA, 2.66 MVA, and 3.55 MVA, respectively. Therefore, combined with actual engineering applications, a comprehensive compensation design scheme for the traction substation can be determined. The device capacity of SVG1, SVG2, and SVG3 can be selected respectively as 3 MVA, 3 MVA, and 5 MVA. Furthermore, the capacity of each device above is the actual value of required to meet the compensation target.

Based on the above compensation design scheme, after implementing the comprehensive compensation of negative sequence and reactive power for the traction substation, the diagram of 24-h device output power of the CCE is shown in Figure 11.

The diagram of 24-h three-phase voltage unbalance degree curve and power factor curve of the traction substation before and after compensation are shown in Figures 12 and 13, respectively.

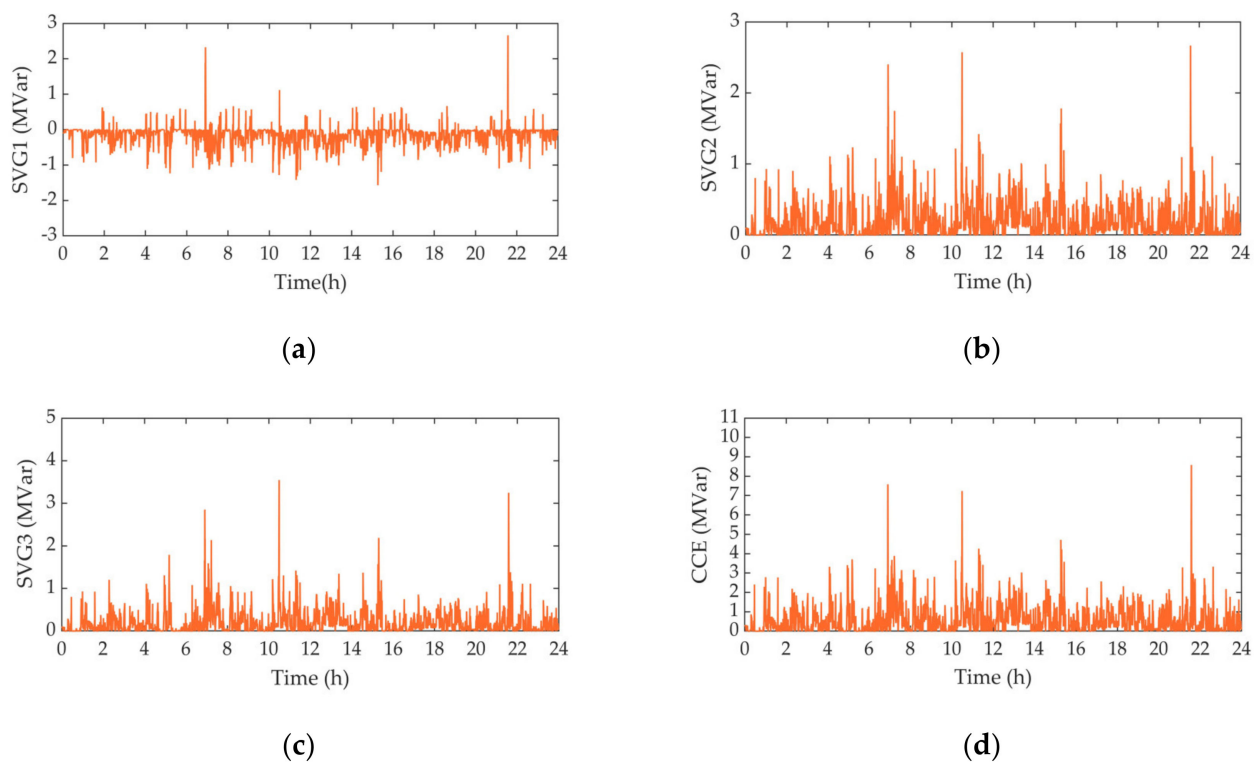


Figure 11. Diagram of device output curve of the CCE during a day. (a) Diagram of device output curve of the Static Var Generator (SVG)1 during a day; (b) diagram of device output curve of the SVG2 during a day; (c) diagram of device output curve of the SVG3 during a day; (d) diagram of total device output curve of the CCE during a day.

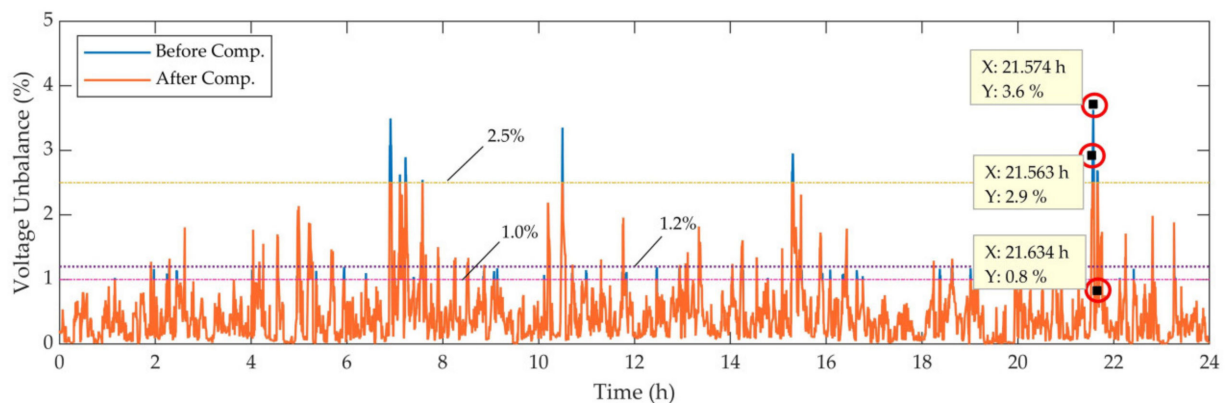


Figure 12. Diagram of 24-h three-phase voltage unbalance degree curve of the traction substation (before and after compensation).

In Figure 14, the statistical result after compensation shows that the 95% probability value of the three-phase voltage unbalance degree of the traction substation has reduced from 1.2% to 1.0%, and the maximum also has reduced from 3.6% to 2.5%. At the same time, the daily average power factor of the traction substation has increased from 0.79 to 0.91, achieving compensation design target.

5.2. Analysis and Verification of Comprehensive Compensation Control Strategy

To verify the effectiveness of the comprehensive compensation control strategy, a simulation model is established with MATLAB/SIMULINK, as shown in Figure 15. In the simulation model, the short-circuit capacity of the power system is set to 500 MVA; on the primary-side of TCT, the power system voltage is 110 kV; on the secondary side of TCT,

the voltage of traction port is 27.5 kV. Furthermore, the constant power source is used for simulating the traction load.

The compensation is only needed when the negative sequence power or reactive power does not meet the requirements of the compensation target. Therefore, based on the actual traction load data within 24 h given in Section 5.1, three typical cases are selected for simulation verification in this section. Among of them, case 1 will conduct simulation analysis for the condition when negative sequence power and reactive power need to be compensated simultaneously; and case 2 will conduct simulation analysis for the condition when only the negative sequence power need to be compensated; finally, case 3 will conduct simulation analysis for the condition when only the reactive power need to be compensated.

Case 1:

In case 1, take the traction load data at 21.574 h as an example, at this time traction the load power is 18.2 MVA, three-phase voltage unbalance degree ε_{U2}^{L1} at the PCC is 3.6%, and power factor $\cos \phi_{L1}$ is 0.8. Because ε_{U2}^{L1} exceeds the limit of 2.5%, and $\cos \phi_{L1}$ is also lower than the limit of economic power factor 0.9. Therefore, according to the comprehensive compensation strategy, comprehensive compensation for negative sequence and reactive power is required. Set the compensation target of three-phase voltage unbalance degree at PCC as $\varepsilon_{U2}^* = 2.5\%$, and power factor compensation target as $\cos \phi^* = 0.9$, so that $K_N = 0.31$, $K_C = 0.35$.

CCE was put into operation at 0.3 s. The simulation results are shown in Figure 16. It can be seen that after CCE operates, the three-phase voltage unbalance degree at the PCC is rapidly reduced from 3.6% to 2.5%. At the same time, the power factor also increased rapidly from 0.8 to 0.9. The compensation target of CCE is realized for negative sequence and reactive power. Table 1 shows the results of case 1 before and after comprehensive compensation.

Case 2:

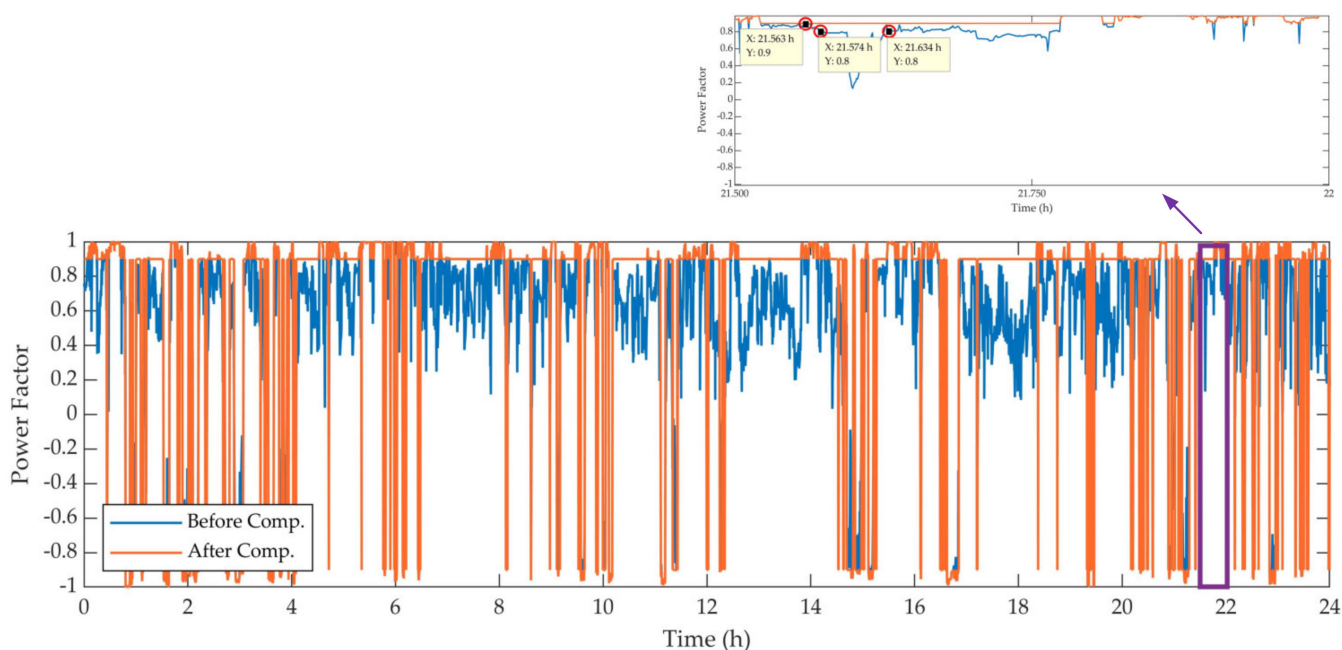


Figure 13. Diagram of 24-h power factor curve of the traction substation (before and after compensation).

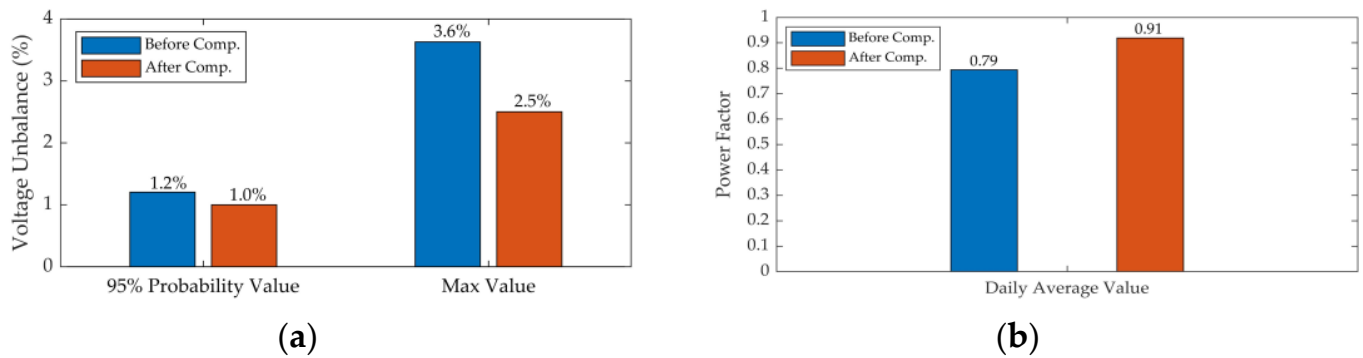


Figure 14. Diagram of statistical result of the data in Figures 12 and 13. (a) Diagram of statistical result of three-phase voltage unbalance degree during a day before and after compensation; (b) diagram of statistical result of power factor during a day before and after compensation.

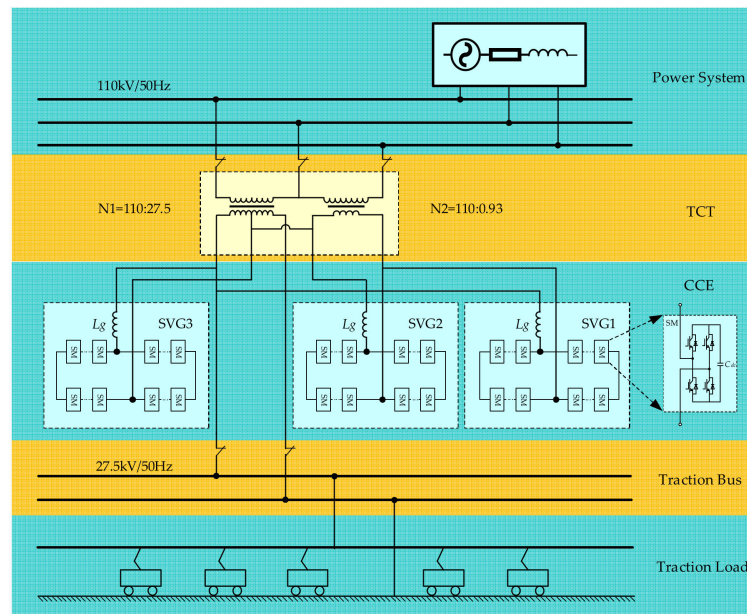


Figure 15. Diagram of comprehensive compensation control strategy simulation.

In case 2, take the traction load data at 21.563 h as an example, at this time traction load power is 14.3 MVA, three-phase voltage unbalance degree ε_{U2}^{L2} at the PCC is 2.9%, and power factor $\cos \phi_{L2}$ is 0.9. Because ε_{U2}^{L2} exceeds the limit of 2.5%, $\cos \phi_{L2}$ still meets the requirement of economic power factor. Therefore, according to the comprehensive compensation control strategy, only the negative sequence power needs to be compensated. Set the compensation target of three-phase voltage unbalance degree at PCC as $\varepsilon_{U2}^* = 2.5\%$, and power factor compensation target as $\cos \phi^* = 0.9$, so that $K_N = 0.31$, $K_C = 0$.

CCE was put into operation at 0.3 s. The simulation results are shown in Figure 17. It can be seen that after CCE operates, the three-phase voltage unbalance degree at the PCC is rapidly reduced from 2.9% to 2.5%. At the same time, because of the CCE does not inject additional reactive power into the system and the reactive power at PCC will not change, the power factor can always be stabilized at 0.9. The compensation target of CCE is realized for negative sequence power. Table 2 shows the results of case 2 before and after negative sequence power compensation.

Case 3:

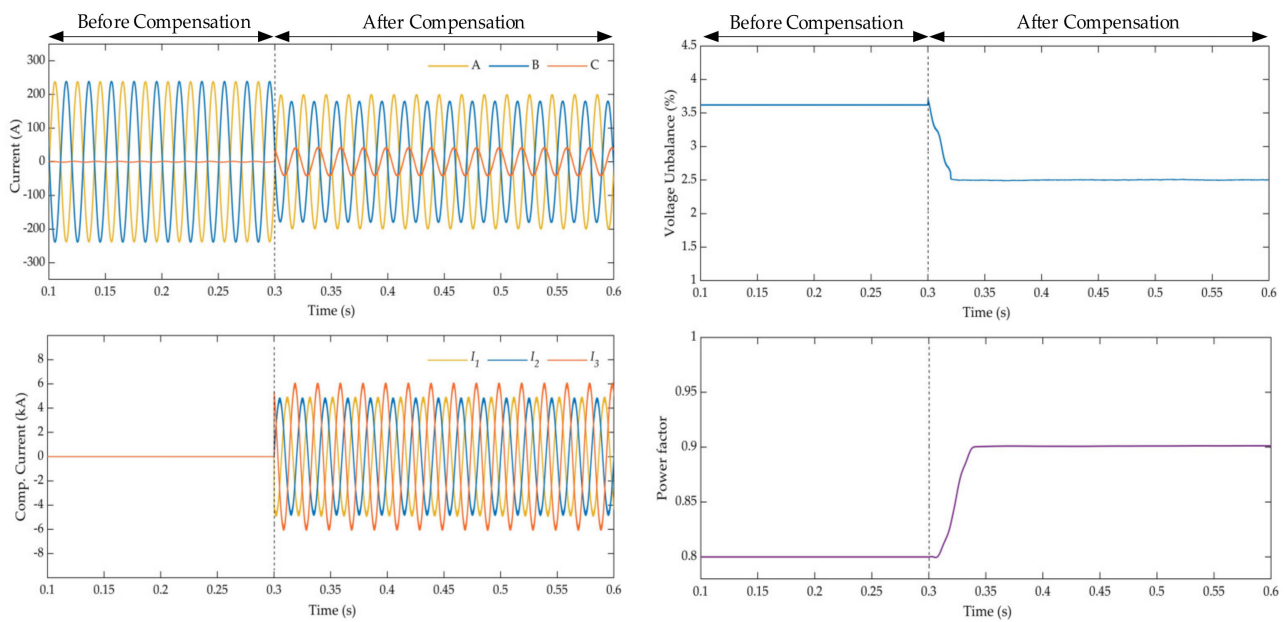


Figure 16. Simulation results at Point of Common Coupling (PCC) before and after comprehensive compensation.

Table 1. Statistical results of typical values before and after comprehensive compensation.

Parameters	Three-Phase Voltage		Three-Phase Voltage Unbalance Degree	Power Factor
	Positive Sequence	Negative Sequence		
Before compensation	61.89 kV	2.23 kV	3.6%	0.8
After compensation	62.28 kV	1.56 kV	2.5%	0.9

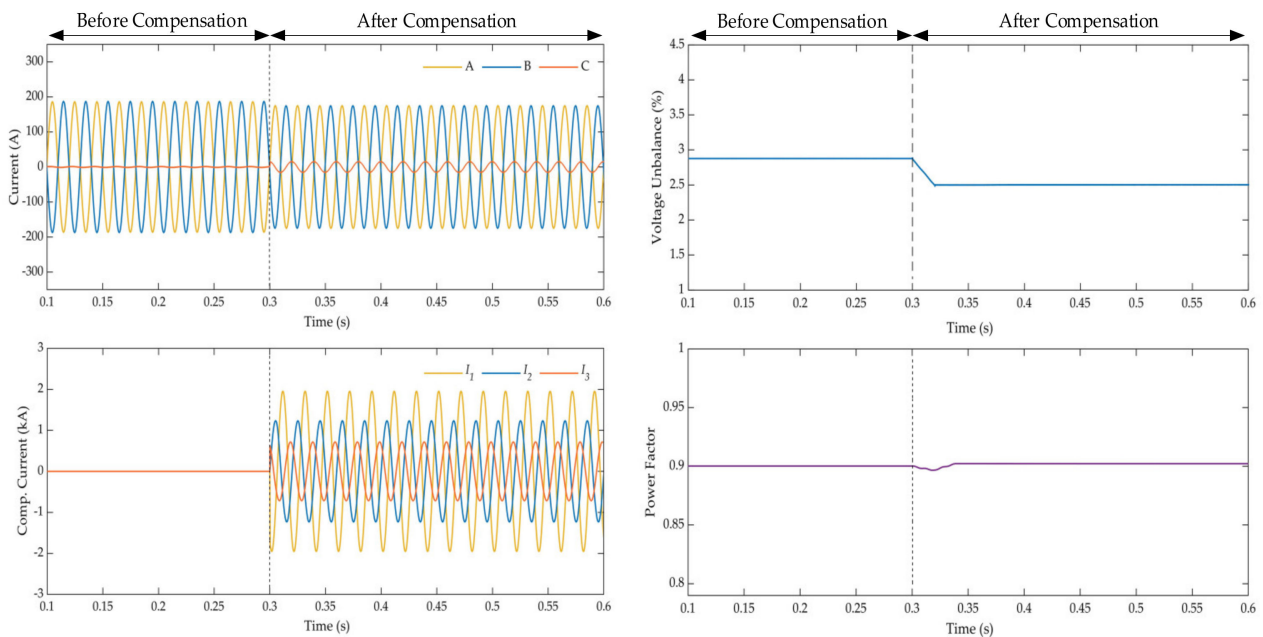


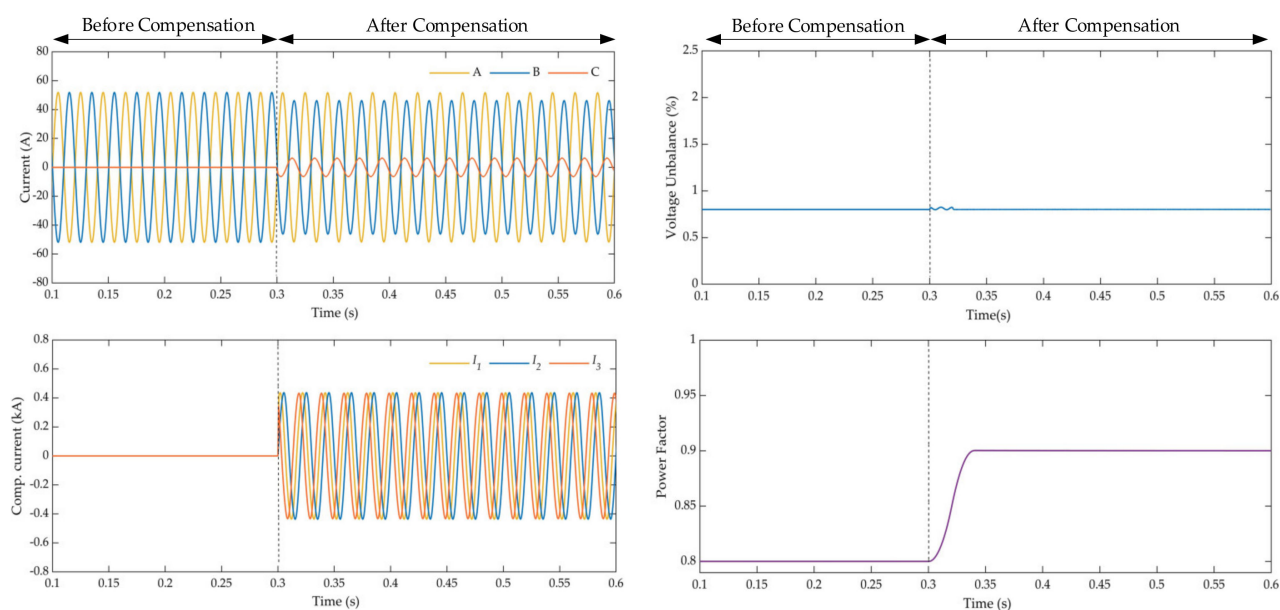
Figure 17. Simulation results at PCC before and after negative sequence power compensation.

Table 2. Statistical results of typical values before and after negative sequence power compensation.

Parameters	Three-Phase Voltage		Three-Phase Voltage Unbalance Degree	Power Factor
	Positive Sequence	Negative Sequence		
Before compensation	62.48 kV	1.80 kV	2.9%	0.9
After compensation	62.48 kV	1.56 kV	2.5%	0.9

In the case 3, take the measured load data of the traction substation at 21.634 h as an example, at this time traction load power is 4.0 MVA, three-phase voltage unbalance degree ε_{U2}^{L3} at the PCC is 0.8%, and power factor $\cos \phi_{L3}$ is 0.9. The other simulation parameters are the same as above. Because ε_{U2}^{L3} meets the 1.0% limit, $\cos \phi_{L3}$ is lower than the limit of economic power factor 0.9. Therefore, according to the comprehensive compensation control strategy, only the reactive power needs to be compensated. Set the compensation target of three-phase voltage unbalance degree at PCC as $\varepsilon_{U2}^* = 0.8\%$, and power factor compensation target as $\cos \phi^* = 0.9$, so that $K_N = 0$, $K_C = 0.35$.

CCE was put into operation at 0.3 s. The simulation results are shown in Figure 18. It can be seen that after CCE operates, the power factor at the PCC is rapidly increased from 0.8 to 0.9. At the same time, the three-phase voltage unbalance degree is always maintained at a low level of 0.8%, and no further compensation for negative sequence power is required. The compensation target of CCE is realized for reactive power. Table 3 shows the results of case 3 before and after reactive power compensation.

**Figure 18.** Simulation results at PCC before and after reactive power compensation.**Table 3.** Statistical results of typical values before and after reactive power compensation.

Parameters	Three-Phase Voltage		Three-Phase Voltage Unbalance Degree	Power Factor
	Positive Sequence	Negative Sequence		
Before compensation	63.15 kV	0.50 kV	0.8%	0.8
After compensation	63.26 kV	0.51 kV	0.8%	0.9

In summary, through the above three simulation experiment results based on measured load data, the effectiveness of the comprehensive compensation control strategy proposed in this paper is fully verified. The system responds quickly and the compensation effect is better.

6. Conclusions

In this paper, a novel co-phase power supply system for electrified railway based on V type connection traction transformer was proposed to cancel neutral section at the outlet of traction substation, and compensate for the negative sequence and reactive power. It is beneficial to reduce the adverse effects caused by the train passing the neutral section and improve the safety of train operation. Moreover, it can also effectively solve the power quality problem mainly caused by the negative sequence power generated by the electrified railway.

The Traction Compensation Transformer (TCT) presented in the scheme has both traction port and compensation port, and the windings of the traction port and compensation port can be shared. It has obvious advantages such as high functional integration, effectively reducing equipment footprint and transformer manufacturing difficulty. Furthermore, the traction port of the TCT is essentially a single-phase transformer with a high capacity utilization rate, which can effectively reduce the installation capacity of the equipment.

The scheme proposed in this paper is suitable for the comprehensive treatment of negative sequence and reactive power of various AC-DC and AC-DC-AC electric locomotives, and the working conditions of the CCE are reversible. When the traction load is working under the regenerative braking conditions, it can still feed power that meets the standard to the power system.

Author Contributions: S.X. proposed the idea, completed the theoretical analysis, and developed the model. Y.Z. collected and analyzed measured data, performed the simulation, and related verification works. S.X., Y.Z. and H.W. wrote the paper. All authors have read and agreed to the published version of the manuscript.

Funding: This work was supported by the National Natural Science Foundation of China (Grant No. 51877182) and the Sichuan Science and Technology Program (Grant No. 2021YJ0028).

Institutional Review Board Statement: Not applicable.

Informed Consent Statement: Not applicable.

Data Availability Statement: Not applicable.

Conflicts of Interest: The authors declare no conflict of interest.

Abbreviations

Abbreviations

SVG	Static Var Generator
PCC	Point of Common Coupling
RPC	Railway Static Power Conditioner
PFC	Power Flow Controller
HPQC	Hybrid Power Quality Conditioner
MMC	Modular Multilevel Converter
SVC	Static Var Compensator
TCT	Traction Compensation Transformer
CCE	Comprehensive Compensation Equipment
MCS	Measurement and Control System
VT	Voltage Transformer
CT	Current Transformer
CD	Controller Device
AT	Auto Transformer

Variables	
$\dot{U}_A, \dot{U}_B, \dot{U}_C$	Voltage of the three-phase high-voltage bus
$\dot{U}_A^-, \dot{U}_B^-, \dot{U}_C^-$	Negative sequence component of $\dot{U}_A, \dot{U}_B, \dot{U}_C$
$\dot{U}_1, \dot{U}_2, \dot{U}_3$	Compensation port voltage of TCT secondary side SVG1, SVG2, SVG3
$\dot{U}_1^-, \dot{U}_2^-, \dot{U}_3^-$	Negative sequence component of $\dot{U}_1, \dot{U}_2, \dot{U}_3$
$\dot{I}_1, \dot{I}_2, \dot{I}_3$	Compensation current generated by SVG1, SVG2, SVG3
$\dot{I}_1^-, \dot{I}_2^-, \dot{I}_3^-$	Negative sequence component of $\dot{I}_1, \dot{I}_2, \dot{I}_3$
\dot{U}_L	Traction port voltage of TCT secondary side
\dot{U}_L^-	Negative sequence component of \dot{U}_L
\dot{I}_L	Traction load current
\dot{I}_L^-	Negative sequence component of \dot{I}_L
Q_{CSS}	Reactive power of co-phase power supply traction substation after compensation
$\cos \phi'_L$	Power factor of co-phase power supply traction substation after compensation
S_L	Total apparent power of traction load
ϕ_L	Power factor angle of traction load
S_k	Reactive power generated by SVGs
ϕ_k	Power factor angle of SVGs
n	The number of compensation ports
K_C	Reactive power compensation degree
ψ_L	Angle of \dot{U}_L lagging behind \dot{U}_A
ψ_k	Angle of compensating port k voltage lagging behind \dot{U}_A
K_N	Negative sequence compensation degree
S_1, S_2, S_3	Reactive power generated by SVG1, SVG2, SVG3
k_L	TCT traction port voltage and primary sideline voltage transformation ratio
k_M	TCT compensation port voltage and primary sideline voltage transformation ratio
I_{L1}	The effective value of fundamental current of traction load
ϕ_{L1}	Power factor angle of fundamental current of traction load
I_{L1p}, I_{L1q}	Instantaneous active component and reactive component of I_{L1}
I_1^*, I_2^*, I_3^*	Expected values of compensation current of SVG1, SVG2, and SVG3
ε_{U2}	The limit of three-phase voltage unbalance degree at PCC
S_ε	The allowable negative sequence power at PCC
S_d	The short circuit capacity at PCC
\dot{S}^-	The residual negative sequence power at PCC after compensation
ε_{U2}^*	Expected value of three-phase voltage unbalance degree at PCC
$\cos \phi^*$	Expected value of power factor

References

- Chen, M.; Chen, Y.; Wei, M. Modeling and Control of a Novel Hybrid Power Quality Compensation System for 25-kV Electrified Railway. *Energies* **2019**, *12*, 3303. [CrossRef]
- He, X.; Ren, H.; Lin, J.; Han, P.; Wang, Y.; Peng, X.; Shu, Z. Power Flow Analysis of the Advanced Co-Phase Traction Power Supply System. *Energies* **2019**, *12*, 754. [CrossRef]
- Railway Statistics Bulletin. 2019. Available online: http://www.gov.cn/xinwen/2020-04/30/content_5507767.htm (accessed on 29 April 2020).
- Femine, A.D.; Gallo, D.; Giordano, D.; Landi, C.; Luiso, M.; Signorino, D. Power Quality Assessment in Railway Traction Supply Systems. *IEEE Trans. Instrum. Meas.* **2020**, *69*, 2355–2366. [CrossRef]
- Chen, Y.; Chen, M.; Tian, Z.; Liu, Y.; Hillmansen, S. VU limit pre-assessment for high-speed railway considering a grid connection scheme. *IET Gener. Transm. Distrib.* **2019**, *13*, 1121–1131. [CrossRef]
- Fang, L.; Xu, X.; Fang, H.; Xiao, Y. Negative-sequence current compensation of power quality compensator for high-speed electric railway. In Proceedings of the 2014 IEEE Conference and Expo Transportation Electrification Asia-Pacific (ITEC Asia-Pacific), Beijing, China, 31 August–3 September 2014; pp. 1–5.
- Tian, X.; Li, X.; Zhou, Z. Novel Uninterruptible Phase-Separation Passing and Power Quality Compensation Scheme Based on Modular Multilevel Converter for Double-Track Electrified Railway. *Energies* **2020**, *13*, 738. [CrossRef]
- Wu, C.; Luo, A.; Shen, J.; Ma, F.; Peng, S. A Negative Sequence Compensation Method Based on a Two-Phase Three-Wire Converter for a High-Speed Railway Traction Power Supply System. *IEEE Trans. Power Electron.* **2012**, *27*, 706–717. [CrossRef]
- He, X.; Shu, Z.; Peng, X.; Zhou, Q.; Zhou, Y.; Zhou, Q.; Gao, S. Advanced Cophase Traction Power Supply System Based on Three-Phase to Single-Phase Converter. *IEEE Trans. Power Electron.* **2014**, *29*, 5323–5333. [CrossRef]

10. Zhou, Y.; Guo, A.; He, X. Output-transformerless traction substation based on three-phase to single-phase cascaded converter. In Proceedings of the 2014 International Power Electronics and Application Conference and Exposition, Shanghai, China, 5–8 November 2014; pp. 749–753.
11. Min, J.; Ma, F.; Xu, Q.; He, Z.; Luo, A.; Spina, A. Analysis, Design, and Implementation of Passivity-Based Control for Multilevel Railway Power Conditioner. *IEEE Trans. Ind. Inf.* **2018**, *14*, 415–425. [[CrossRef](#)]
12. Luo, A.; Ma, F.; Wu, C.; Ding, S.; Zhong, Q.; Shuai, Z. A Dual-Loop Control Strategy of Railway Static Power Regulator Under V/V Electric Traction System. *IEEE Trans. Power Electron.* **2011**, *26*, 2079–2091. [[CrossRef](#)]
13. Zhang, D.; Zhang, Z.; Wang, W.; Yang, Y. Negative Sequence Current Optimizing Control Based on Railway Static Power Conditioner in V/v Traction Power Supply System. *IEEE Trans. Power Electron.* **2016**, *31*, 200–212. [[CrossRef](#)]
14. Ma, F.; Xu, Q.; He, Z.; Tu, C.; Shuai, Z.; Lou, A.; Li, Y. A Railway Traction Power Conditioner Using Modular Multilevel Converter and Its Control Strategy for High-Speed Railway System. *IEEE Trans. Transp. Electr.* **2016**, *2*, 96–109. [[CrossRef](#)]
15. Chen, M.; Liu, R.; Xie, S.; Zhang, X.; Zhou, Y. Modeling and Simulation of Novel Railway Power Supply System Based on Power Conversion Technology. In Proceedings of the 2018 International Power Electronics Conference (IPEC-Niigata 2018-ECCE Asia), Niigata, Japan, 20–24 May 2018; pp. 2547–2551.
16. Zhu, X.; Chen, M.; Xie, S.; Luo, J. Research on new traction power system using power flow controller and Vx connection transformer. In Proceedings of the 2016 IEEE International Conference on Intelligent Rail Transportation (ICIRT), Birmingham, UK, 23–25 August 2016; pp. 111–115.
17. Kaleybar, H.J.; Brenna, M.; Foadelli, F.; Fazel, S.S. Regenerative Braking Energy and Power Quality Analysis in 2×25 kV High-Speed Railway Lines Operating with 4QC Locomotives. In Proceedings of the 2020 11th Power Electronic and Drive Systems and Technologies Conference (PEDSTC), Tehran, Iran, 4–6 February 2020; pp. 1–6.
18. Mariscotti, A. Behaviour of Spectral Active Power Terms for the Swiss 15 kV 16.7 Hz Railway System. In Proceedings of the 2019 IEEE 10th International Workshop on Applied Measurements for Power Systems (AMPS), Aachen, Germany, 25–27 September 2019; pp. 1–6.
19. Li, Q. New generation traction power supply system and its key technologies for electrified railways. *J. Mod. Transport.* **2015**, *23*, 1–11. [[CrossRef](#)]
20. Mochinaga, Y.; Hisamizu, Y.; Takeda, M.; Miyashita, T.; Hasuike, K. Static power conditioner using GTO converters for AC electric railway. In Proceedings of the Power Conversion Conference, Yokohama, Japan, 19–23 April 1993; pp. 641–646.
21. Mochinaga, Y.; Uzuka, T. Development of Single Phase Feeding Power Conditioner for Shinkansen Depots. *QR RTRI* **2000**, *41*, 154–158. [[CrossRef](#)]
22. Morimoto, H.; Ando, M.; Mochinaga, Y.; Kato, T.; Yoshizawa, J.; Gomi, T.; Miyashita, T.; Funahashi, S.; Nishitoba, M.; Oozeki, S. Development of railway static power conditioner used at substation for Shinkansen. In Proceedings of the Power Conversion Conference, Osaka, Japan, 2–5 April 2002; pp. 1108–1111.
23. Li, Q.; Zhang, J.; He, W. Research on a new power supply system suitable for heavy-duty electric traction. *J. CRS* **1988**, *4*, 23–31. (In Chinese)
24. Li, Q. Unified traction power supply mode for trunk railway and urban rail transit. *Sci. Sin. Tech.* **2018**, *48*, 1179–1189. (In Chinese) [[CrossRef](#)]
25. Li, Q. Several Key Technical Issues in the Development of Traction Power Supply for High-speed Railways in China. *J. CRS* **2010**, *32*, 119–124. (In Chinese)
26. Shu, Z.; Xie, S.; Li, Q. Single-Phase Back-To-Back Converter for Active Power Balancing, Reactive Power Compensation, and Harmonic Filtering in Traction Power System. *IEEE Trans. Power Electron.* **2011**, *26*, 334–343. [[CrossRef](#)]
27. Shu, Z.; Xie, S.; Lu, K.; Zhao, Y.; Nan, X.; Qiu, D.; Zhou, F.; Gao, S.; Li, Q. Digital Detection, Control, and Distribution System for Co-Phase Traction Power Supply Application. *IEEE Trans. Ind. Electron.* **2013**, *60*, 1831–1839. [[CrossRef](#)]
28. He, X.; Guo, A.; Peng, X.; Zhou, Y.; Shi, Z.; Shu, Z. A Traction Three-Phase to Single-Phase Cascade Converter Substation in an Advanced Traction Power Supply System. *Energies* **2015**, *8*, 9915–9929. [[CrossRef](#)]
29. Lao, K.; Wong, M.; Dai, N.Y.; Wong, C.; Lam, C. Analysis of DC-Link Operation Voltage of a Hybrid Railway Power Quality Conditioner and Its PQ Compensation Capability in High-Speed Cophase Traction Power Supply. *IEEE Trans. Power Electron.* **2016**, *31*, 1643–1656. [[CrossRef](#)]
30. Habibolahzadeh, M.; Roudsari, H.M.; Jalilian, A.; Jamali, S. Improved Railway Static Power Conditioner Using C-type Filter in Scott Co-phase Traction Power Supply System. In Proceedings of the 2019 10th International Power Electronic and Drive Systems and Technologies Conference (PEDSTC), Shiraz, Iran, 12–14 February 2019; pp. 355–360.
31. Vemulapati, V.; Vijayakumar, Y.N.; Visali, N. Droop Characteristics based High Speed Traction Power Supply system using Modular Multilevel Converter. In Proceedings of the 2020 4th International Conference on Trends in Electronics and Informatics (ICOEI), Tirunelveli, India, 15–17 June 2020; pp. 111–118.
32. Vijaykumar, Y.N.; Vemulapati, V.; Visali, N.; Raju, K. Railway Power Supply System using Modular Multilevel Converter with Droop Characteristics. In Proceedings of the 2020 4th International Conference on Electronics, Communication and Aerospace Technology (ICECA), Coimbatore, India, 5–7 November 2020; pp. 12–20.
33. AlBader, M.; Enjeti, P. Three phase to Co-phase railway electrification approach using voltage synthesizing electronic phase shifter (EPS). In Proceedings of the 2016 IEEE Transportation Electrification Conference and Expo (ITEC), Dearborn, MI, USA, 27–29 June 2016; pp. 1–4.

-
34. Mousavi Gazafrudi, S.M.; Tabakhpour Langerudy, A.; Fuchs, E.F.; Al-Haddad, K. Power Quality Issues in Railway Electrification: A Comprehensive Perspective. *IEEE Trans. Ind. Electron.* **2015**, *62*, 3081–3090. [[CrossRef](#)]
 35. Omi, M.; Kotegawa, R.; Ando, M.; Masui, T.; Horita, Y. Introduction and effectiveness of STATCOM to the independent power system of JR East. In Proceedings of the 2014 International Power Electronics Conference (IPEC-Hiroshima 2014-ECCE ASIA), Hiroshima, Japan, 18–21 May 2014; pp. 1317–1321.
 36. Tamai, S. Novel power electronics application in traction power supply system in Japan. In Proceedings of the 2014 16th International Power Electronics and Motion Control Conference and Exposition, Antalya, Turkey, 21–24 September 2014; pp. 701–706.
 37. Luo, L.; Chen, P.; Cui, P.; Zhang, Z.; Zhou, Y.; Xie, X.; Chen, J. A current balance compensation method for traction substation based on SVG and V/v transformer. In Proceedings of the 2017 IEEE Transportation Electrification Conference and Expo, Asia-Pacific (ITEC Asia-Pacific), Harbin, China, 7–10 August 2017; pp. 1–6.
 38. Horita, Y.; Morishima, N.; Kai, M.; Onishi, M.; Masui, T.; Noguchi, M. Single-phase STATCOM for feeding system of Tokaido Shinkansen. In Proceedings of the 2010 International Power Electronics Conference-ECCE ASIA, Sapporo, Japan, 21–24 June 2010; pp. 2165–2170.
 39. Li, Q.; He, J. *Analysis of Traction Power Supply System*; Southwest Jiaotong University Press: Chengdu, China, 2012.
 40. *Power Quality—Three-Phase Voltage Unbalance*; National Standard of the People's Republic of China GB/T 15543-2008; Standardization Administration of the People's Republic of China: Beijing, China, 2008.